

Thermodynamic description of reactions between Mg and CaO

Rainer Schmid-Fetzer¹, Artem Kozlov¹, Björn Wiese², Chamini L. Mendis², Domonkos Tolnai², Karl U. Kainer², Norbert Hort²

¹Institute of Metallurgy, Clausthal University of Technology, Robert-Koch-Str. 42,
D-38678 Clausthal-Zellerfeld, Germany
schmid-fetzer@tu-clausthal.de

²Magnesium Innovation Centre, Helmholtz-Zentrum Geesthacht,
Max Planck Straße 1, D-21502 Geesthacht, Germany

Keywords: Magnesium alloys, CaO, *in situ* XRD, thermodynamic evaluation

Abstract

CaO is considered as possible replacement for cover gases such as SF₆ during melting and casting of Mg alloys. Such CaO additions to molten Mg increase the ignition resistance by forming a protective oxide layer. The actual reactions between liquid Mg and CaO are not well understood. An approach based on chemical reaction equations cannot capture the "CaO dissolution" process. This work presents the development of a consistent thermodynamic description of the ternary Mg-Ca-O alloy system. To that end a revision of the thermodynamic data of key oxides, CaO and MgO, has been performed based on original experimental work so far not considered in thermodynamic databases or tabulations. The formation of a liquid Mg-Ca-[O] alloy during the reaction is predicted from the thermodynamic calculations at melting temperatures; solidification simulations are also performed. These predictions from thermodynamic simulations are validated by experimental data using *in situ* synchrotron radiation diffraction.

Introduction

CaO is used as a cheaper replacement for pure Ca as an alloying addition in Mg alloys. The main motivation for the use of CaO is to reduce the use of cover gases such as SF₆ during melting and casting of Mg alloys. A new group of alloys named as ECO-Mg (Environment CONscious magnesium) with Ca additions to achieve this has been developed [1]. The CaO dissociation (or reduction) in Mg and Mg alloys is reported in literature, but no or insufficient explanation is given [2-4]. According to the Ellingham diagram CaO is more stable than MgO at temperatures of interest [5, 6], therefore, it is often expected that CaO remains unreacted during melting of Mg. In contrast, it is observed that CaO dissolves during the melting procedure [2, 3] and has a protective effect on Mg melts [7-9].

Kondoh et al. [4] proposed a calculation to explain the disassociation of CaO in Mg-Al alloys. They used tabulated Gibbs energy data for the reaction between pure Mg (plus pure Al) and CaO. As reaction products MgO and Ca or the Laves phases, Mg₂Ca and Al₂Ca, were considered. Their key finding is that pure Mg cannot react with CaO because of a positive Gibbs energy of reaction. Experimental results for the stability of Mg + CaO were also mentioned but not presented [4]. They only presented results for the reaction of a Mg-Al-Zn alloy, AZ61B, mixed in different ratios with CaO. In this case CaO was reduced, essentially because Al₂Ca may form.

Gourishankar et al. [10] measured the Gibbs energy and enthalpy of formation, ΔH° , for CaO and MgO. Their derived values for $\Delta H^\circ(298\text{ K})$ of CaO and MgO are -602 and -635 kJ/mol, respectively. This differs significantly from the JANAF-tables [6] by +33 kJ/mol for CaO and -34 kJ/mol for MgO. This is

important because, in this case, MgO and CaO swap the positions in the Ellingham diagram. These data published in 1993 [10], however, have never been acknowledged in any recent tabulated thermodynamic data compilation [11-13] or the leading electronic databases for pure substances, SGTE [14] or FactPS [15] or Calphad assessments of oxide systems [16].

In addition to this problem with the oxide data it will be shown that the approach based on chemical reaction equations cannot capture the "CaO dissolution" process. That is because multicomponent solution phases, especially liquid, will govern the reaction. The purpose of this work is to demonstrate that the Mg + CaO reaction can only be understood by development of a consistent thermodynamic description of the ternary Mg-Ca-O alloy system and phase diagram. These calculations are verified by dedicated experimental investigation of the Mg + CaO reactions and the subsequent alloy solidification.

Experimental procedure

Sample preparation

The sample Mg₂₀CaO was prepared from chips of pure Mg (99.9 %) and CaO powder (Calcium oxide $\geq 96\%$ powder from CARL ROTH). The nominal composition of the sample investigated was Mg + 20 wt.% CaO. The CaO was dried for 6 h at 350°C and mixed with Mg chips for 3 min to achieve a uniform mixture. The mixture was pressed with a hydraulic press to cylinders (diameter of 4 mm and a height of 3 mm) with an applied pressure was 100 MPa and held for 1 min under pressure.

In situ synchrotron radiation diffraction measurement

The *in situ* studies were conducted at P07 hutch of the High Energy Materials Science (HEMS) beam line at PETRA III [17, 18] at DESY (Deutsches Elektronen-Synchrotron) in Hamburg Germany. The synchrotron radiation diffraction study was conducted with a beam energy of 100 keV, ($\lambda = 0.0124\text{ nm}$) in transmission geometry with a beam cross section of 1x1 mm².

The sample was heated in an Ar atmosphere to 750°C at 10 K/min, held at 750°C for 5 min to ensure melt homogeneity, and then cooled at 10 K/min to 200°C (fully solidified state) before air-cooling to room temperature. The molten samples were held in position in an inverted graphite crucible with a steel lid. The temperature-time-curve was controlled with an S type thermocouple welded to the lid of the crucible. The crucible with sample was rotated by 90° during acquisition to improve statistics. The two dimensional (2D) diffraction patterns were recorded every 12 s at an acquisition time of 1 s with a PerkinElmer XRD 1622 Flatpanel at a sample-to-detector-distance of 1162.7 mm (calibrated with LaB₆ reference). The temperature resolution of the measurement was 2 K. X-ray line profiles were obtained by azimuthal integration of the 2D diffraction patterns through 360° using FIT2D V12.077 software. For phase identification

simulated line profiles were generated with CaRIne 3.1 Crystallography™ with crystal structure data from the Pearson's Crystallography Database [19].

Measurement of O content of Mg chips

For this measurement the chips were pressed with a hydraulic press to cylinders with a diameter of 4.0 mm, under an applied pressure of 500 MPa and held for 1 min under pressure. The Mg and O content was measured with a TESCAN VEGA III, equipped with an EDAX energy-dispersive X-ray spectrometer (EDXS) operating at 20 kV. Three separate measurements were made with EDXS for 10 min.

Metallographic investigation

The specimens for SEM were prepared by grinding with SiC paper to 2500 grit at a speed of 150 min⁻¹. Samples were then polished in a 3 μm diamond suspension followed with a mixture of 1 μm diamond suspension and OPS™ (≈ 0.1 μm) anhydrous suspension.

Microstructures were analyzed with SEM (TESCAN VERGA III) and the local compositions were determined with EDXS compositional maps. The compositional maps are recalculated with the software Iridium Ultra in wt.%.

Experimental Results

In situ synchrotron radiation diffraction

The X-ray line profiles for selected temperatures, integrated from 2D diffraction patterns recorded during solidification experiments, are shown in Figure 1 and the pertinent temperatures at which phase transformations are detected are listed in Table I and the line profiles (LP) at different temperatures are illustrated in Fig. 1.

Table I: Temperatures where various phase transformation were observed during solidification of Mg20CaO.

Reaction	Experimental data ± 5 [°C]
Appearance of Mg start	570
Appearance of Mg ₂ Ca start	511
Appearance of Mg end	509
Appearance of Mg ₂ Ca end	509

The X-ray line profiles show that peaks due to Ca[OH]₂, CaO, Mg and graphite crucible are present in the beginning of the experiment. During heating the main peak of CaO becomes more visible when heated above 291°C, due to the thermal expansion of Mg. This is followed by the stabilisation of the intensity of CaO peaks up to 396°C and a second increase in the peak intensity was observed at 502°C to a maximum of intensity. The intensity of CaO decreased as the sample was heated above 568°C. During heating the peaks of MgO are detected initially at 368°C. The peaks of Ca[OH]₂ starts to disappear at 408°C and are undetectable at 500°C. The MgO peaks did not increase further beyond 618°C. In the range between 620 and 637°C the Mg peaks disappear. With the disappearance of solid Mg the diffuse signal of the melt was detected. From a temperature of 664°C the CaO peaks stabilize and show no significant changes in intensity.

During cooling the first peaks of Mg are detected at 570°C and no intensity changes were detected below 509°C. The Laves phase Mg₂Ca was detected at 511°C with no further intensity changes below 509°C.

As the samples were rotated during the measurement results are not limited to single view of the sample but provide better statistics on the amount of various phases.

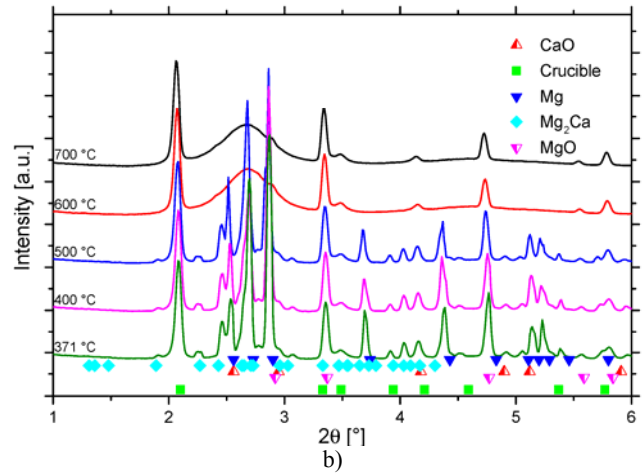
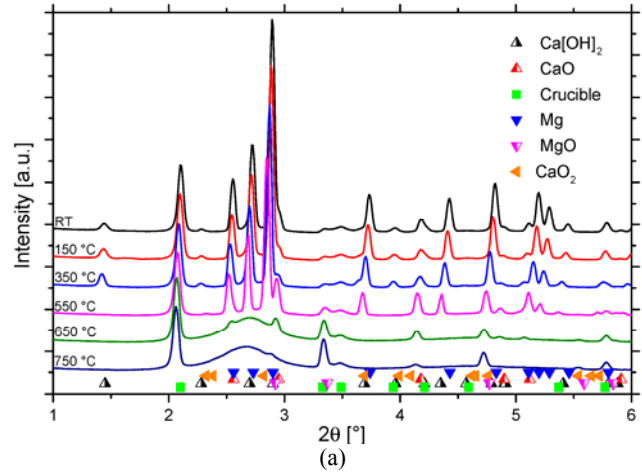


Figure 1: Selected line profiles during a) heating and b) cooling of the Mg20CaO sample with the identity of detected phases.

Microstructures of the solidified samples

The microstructure of the sample used for *in situ* investigations was analyzed with SEM. The EDXS maps show the distribution of the Mg, Ca and O in the as-solidified sample in Fig. 2. From the microstructure the solidification sequence can be understood. The solidification begins with Mg grains and ends finally with the eutectic solidification of an Mg- and Ca-rich lamellar structure. The O agglomerates in the eutectic as clusters of oxide particles with a higher concentration of Mg compared to the intermetallic phase. The composition of the as-solidified sample was measured with EDXS to be 6.8 wt.% Ca, 8.7 wt.% O and balance Mg. This composition deviates from the nominal content of 14.3 wt.% Ca, 5.7 wt.% O and balance Mg.

The composition of the pure Mg chips, measured by EDXS, was 97.73±0.23 wt.% Mg and 2.27±0.23 wt.% O.

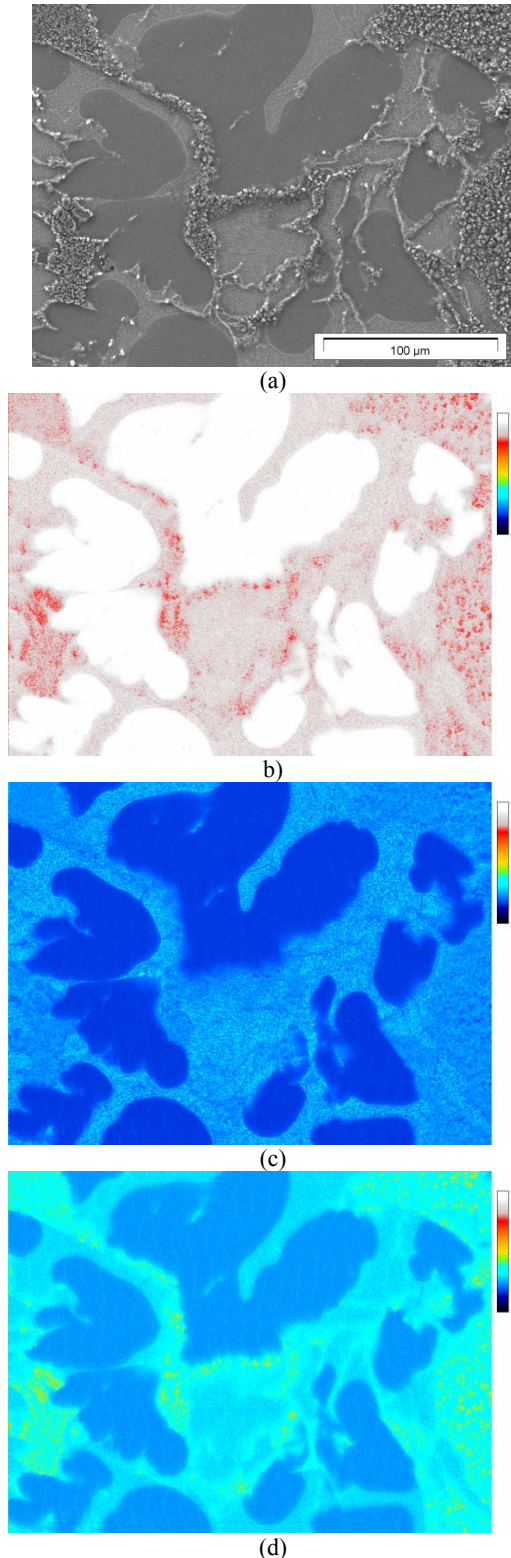


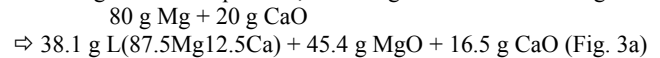
Figure 2: The SE microstructure (a) and EDXS maps for (b) Mg, (c) Ca and (d) O of the Mg₂₀CaO sample, composition in wt.%.

Thermodynamic description of reactions in the ternary Mg-Ca-O system

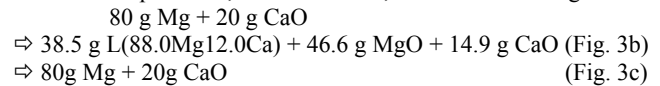
Two thermodynamic databases of the ternary Mg-Ca-O system were developed in this study. Both are based on the thermodynamic functions on the well established Mg-Ca alloy system and the gas phase from the PanMg2014 database [20]. Two different sets of Gibbs energy functions for the solid oxides, MgO, CaO, and CaO₂, were incorporated. In the first database the currently established data from the leading electronic databases for pure substances, SGTE [14] or FactPS [15] with the numerical values given in [16] were used. In the second database a refined version of the Gibbs energy functions for the solid oxides, based on experimental data from [10], was used and more details of this development will be presented elsewhere [21]. All calculations were done using the Pandat software package [22].

The ternary phase diagrams at 700, 600, and 500°C calculated from the first database are shown in Fig. 3, those calculated from the latter, which are accepted as correct ones in this work, in Fig. 4. The oxide CaO₂ is not stable at these temperatures. The single-phase regions of liquid are shown as thick blue lines for easy reading, the quantitative oxygen solubility in Mg-Ca alloys is negligible on this scale.

The basic idea of clearly understanding any reaction of Mg with CaO by reading these phase diagrams is explained for the nominal composition of sample Mg₂₀CaO, indicated by the solid red dot. In Fig. 3a, at 700°C, this dot is located in the three-phase equilibrium L + MgO + CaO, thus, CaO will be partly reduced. The calculated liquid composition is 87.5Mg12.5Ca (wt.%). The equilibrium phase fractions, also obtained by applying the lever rule to this tie-triangle, are presented in the following "reaction equation", assuming a total mass of 100 g:

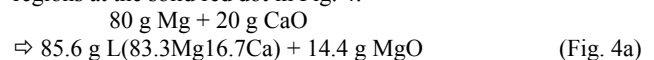


At lower temperatures, 600 and 500°C, we obtain from Figs. 3b-c:

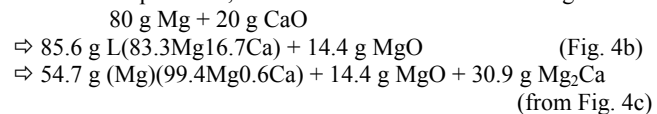


That is, after completion of solidification, Mg and CaO should not react if the currently established oxide data were correct.

In contrast, the second thermodynamic database developed and accepted as correct one in this work gives the following results that can be read from the equilibrium phase regions at the solid red dot in Fig. 4:



At lower temperatures, 600 and 500°C we obtain from Figs. 4b-c:



Thus, CaO will be completely reduced at all temperatures, forming MgO and Mg-rich liquid or, after solidification, Mg₂Ca and (Mg) solid solution.

It is obvious from this simple example that any approach based on classical chemical reaction equations cannot capture the "CaO dissolution" process. The composition of the liquid phase forming would be unknown without the phase diagrams and it will change with temperature. Moreover, for different Mg/CaO initial ratios the results are easily read from the ternary phase diagrams because the solid red dot just shifts along the mass balance line connecting Mg and CaO. It will, thus, fall in the corresponding phase regions in Figs. 3 or 4, clearly indicating the assembly of equilibrium products. Without these phase diagrams one would have no clue how to write down classical

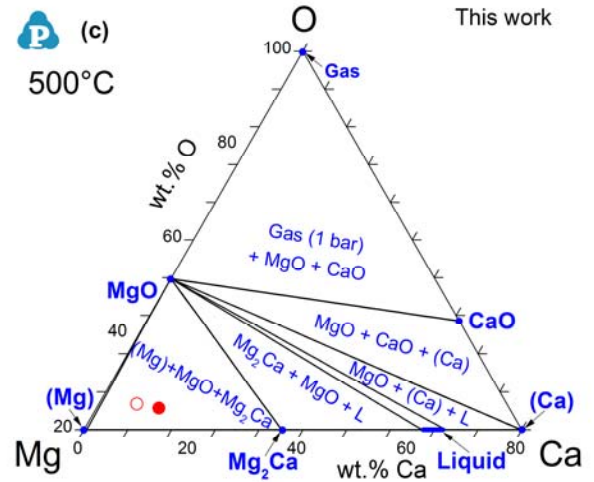
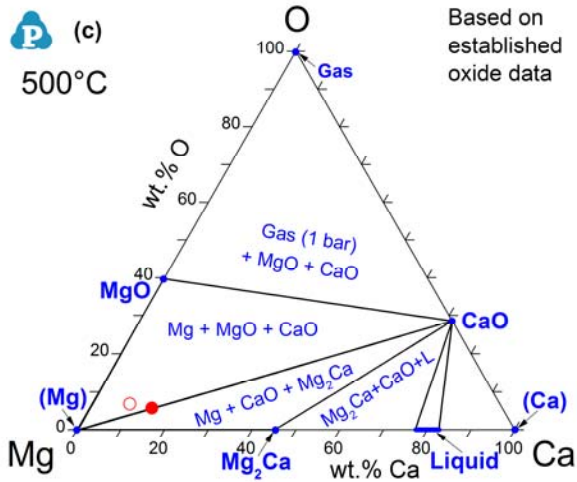
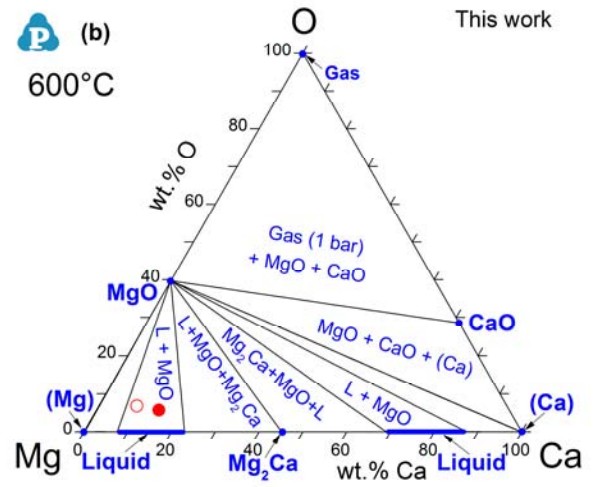
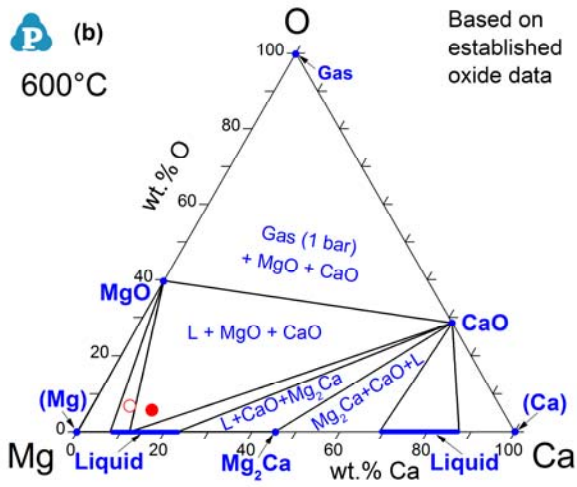
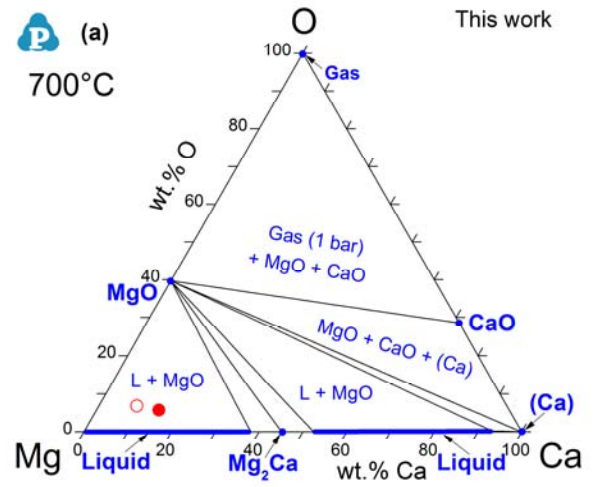
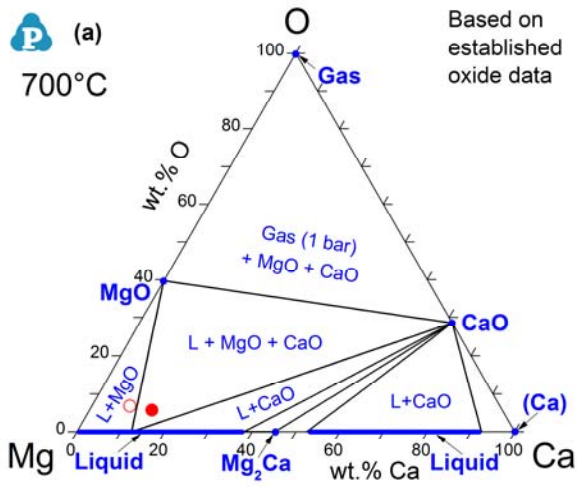


Figure 3: Calculated isothermal sections of the Mg-Ca-O phase diagram from the first thermodynamic database constructed using oxide data [16] established in current literature; (a) 700°C, (b) 600°C, (c) 500°C; the solid red dot indicates the nominal sample composition $Mg_{20}CaO$ and the open circle its composition measured by EDXS.

Figure 4: Calculated isothermal sections of the Mg-Ca-O phase diagram from the second thermodynamic database, developed using oxide data from [10] in this work [21]; (a) 700°C, (b) 600°C, (c) 500°C; the solid and open red circles are the same as in Fig. 3.

chemical reaction equations, which also need to be different for any temperature and Mg/CaO initial ratio, as seen from the six example "equations" above.

It is further emphasized that consideration of binary phase diagrams only, as tried by Kondoh et al. [4], is not viable. The equilibrium phase assembly is governed by the tie line distribution in the ternary phase diagrams as shown in Figs. 3 and 4. The two thermodynamic databases differ essentially in the result that a tie line between Mg-rich metallic phase and CaO does not exist at any temperature in Fig. 4, in contrast to Fig. 3.

Discussion of reactions and solidification of sample Mg20CaO

The experimentally observed results in this work can be discussed best by comparison with calculated equilibrium phase fractions of sample Mg20CaO as shown in Fig. 5.

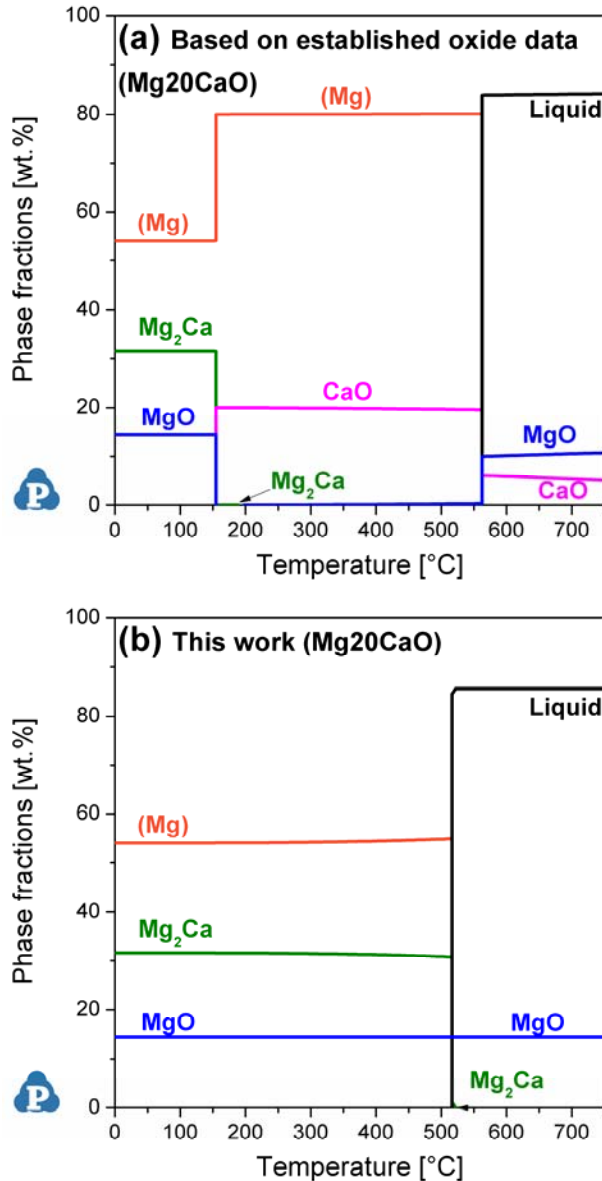


Figure 5: Calculated equilibrium phase fractions for the nominal composition of sample Mg20CaO, Mg-14.3Ca-5.7O (wt.%); (a) Using the first database, see Fig. 3, (b) Using the second database, accepted in this work, see Fig. 4.

Using the first thermodynamic database, Fig. 5a shows that for example at 500°C the sample should consist of 80% (Mg) and 20% CaO. That is consistent with Fig. 3c and the lever rule applied to the solid red dot, the nominal sample composition. That, however, is in stark contrast to the experimental result demonstrating that after melting and equilibration the initially strong XRD signals of CaO essentially disappear and dominant signals of MgO appear. Moreover, the formation of Mg₂Ca is predicted below 200°C only, in a solid state reaction, by using the first database. That is again in conflict with the experimental finding that Mg₂Ca is formed from the liquid phase during solidification, starting at 511°C. This disapproves the validity of the first database.

In contrast, the second database correctly predicts in Fig. 5b that CaO is completely reduced and MgO forms as equilibrium phase at all temperatures. It also correctly predicts the formation of significant amount of Mg₂Ca (30%) from the liquid phase in a eutectic reaction $L = (Mg) + Mg_2Ca (+MgO)$ at 516.5°C. This invariant four-phase reaction is degenerate to the binary Mg-Ca because of the negligible content of oxygen in liquid, thus, the amount of 14.4% MgO remains unchanged in that eutectic. As a detail in Fig. 5b, it is seen that a small amount of 0.9% Mg₂Ca should crystallize as primary phase below 522°C, which is not observed in the microstructure, Fig. 2.

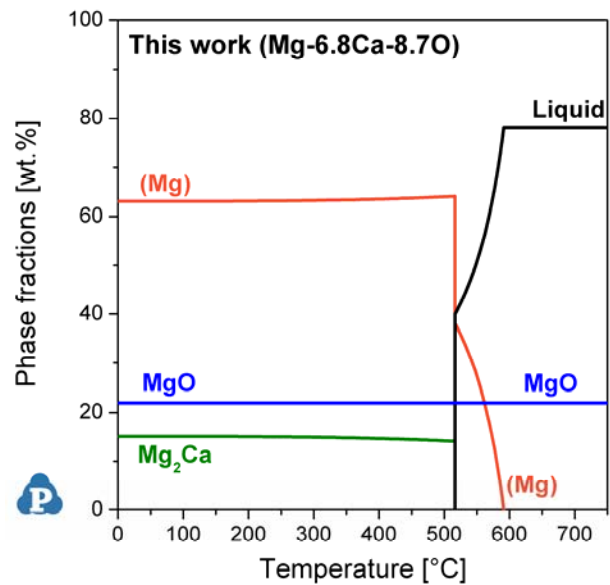


Figure 6: Calculated equilibrium phase fractions for the composition of sample Mg20CaO measured by EDXS, Mg-6.8Ca-8.7O (wt.%) using the second thermodynamic database, accepted in this work, see Fig. 4.

This leads us to the calculated phase fractions of the shifted sample composition Mg-6.8Ca-8.7O (wt.%), measured by EDXS and marked by the open symbol in Fig. 4, using the second thermodynamic database. At this sample composition primary crystallization of (Mg) is predicted to start at 591°C from the liquid with composition L(91.3Mg8.7Ca). That is consistent with the experimental finding of primary (Mg) by *in situ* XRD, and microstructure observation, Fig. 2. The temperature for start of (Mg) in Table I, 570°C, is somewhat below the predicted value. However, the accuracy of the EDXS measurement has also to be taken into account. Thermodynamic calculations reveal that for an

assumed liquid composition L(88.9Mg11.1Ca) an exact match of the primary (Mg) precipitation at 570°C is obtained. That corresponds to a shifted sample composition of Mg-6.8Ca-15.3O or Mg-8.3Ca-10.0O (wt.%), or any point along the tie line L(88.9Mg11.1Ca) + MgO, they all show primary (Mg) at 570°C.

It is seen from Fig. 4a that any initial Mg/CaO mixture with overall composition inside the L + MgO region will react to these two phases by melting at 700°C. The composition of the Mg-Ca liquid that forms is obtained by plotting the tie line from MgO to L that cuts through the initial composition point. Inevitably, the Mg-content of L will be higher than that of the initial mixture.

That construction also reveals that any initial mixture located on that same tie line forms the same liquid composition, just the MgO/L phase amount ratio changes. The amount of MgO formed during melting and equilibration will remain constant during the subsequent solidification of that essentially binary Mg-Ca liquid.

For the alloy compositions with reduced Ca-content compared to the nominal one, such as the EDXS value assumed in Fig. 6, the calculation with the second database also correctly predicts the formation of Mg₂Ca in a eutectic microstructure observed clearly in the fine lamellar structure of Fig. 2a and the corresponding composition values of Figs 2b-c. Specifically, this is the degenerate eutectic reaction $L = (Mg) + Mg_2Ca (+MgO)$ at 516.5°C. The experimentally observed temperature from *in situ* XRD measurements in Table I, 511°C, is somewhat lower and may be due to some non-equilibrium undercooling but is still in agreement within experimental accuracy. It is also confirmed that Mg₂Ca forms in an invariant reaction, given the small spread of only 2 K between start and end of Mg₂Ca signal appearance. This final eutectic solidification step is also confirmed by the disappearance of the diffuse signal from the molten metal.

Conclusion

Dedicated thermodynamic calculations and experimental work reveal that:

- The previously claimed stability of pure Mg with CaO [4] and thermodynamic data of CaO and MgO currently considered established [14, 15] are disproved.
- In a Mg + 20 wt.% CaO sample the CaO is reduced during melting. The microstructure of the solidified sample resembles that of a binary Mg-Ca liquid with finely dispersed MgO particles.
- The Mg + CaO reactions cannot be understood by classical chemical reaction equations but only through the ternary Mg-Ca-O phase diagrams.
- The second thermodynamic database developed in this work correctly predicts these reactions during melting and subsequent solidification. It is implemented in the updated version of the PanMg database [20], PanMg2015.
- This approach enlightens the CaO "dissolution" in Mg melts and the protective effect of CaO on Mg melts.

Acknowledgment

The authors acknowledge the Deutsches Elektronen-Synchrotron for the provision of access to the synchrotron radiation facilities in the framework of the proposal I-20130330.

References

1. Shae K. Kim, "Design and Development of High-Performance Eco-Mg Alloys", in *Magnesium Alloys - Design, Processing and Properties*, ed. F. Czerwinski (InTech, Rijeka, Croatia, 2011) 431-468.
2. S.-H. Ha et al., "Behavior of CaO and Calcium in Pure Magnesium," *Rare Metals*, 25 (2006), 150-154.
3. S.-H. Ha, J.-K. Lee, S. K. Kim, "Effect of CaO on Oxidation Resistance and Microstructure of Pure Mg," *Mater. Trans.*, 49 (2008), 1081-1083.
4. K. Kondoh et al., "Thermo-dynamic analysis on solid-state reduction of CaO particles dispersed in Mg-Al alloy," *Mater. Chem. Phys.*, 129 (2011), 631-640.
5. I. Barin, O. Knacke, and O. Kubaschewski, *Thermochemical properties of inorganic substances, Volume 1* (Springer-Verlag Berlin, Heidelberg, 1977) 861.
6. M. W. Chase et al., *JANAF Thermochemical Tables Third Edition, Volume 14* (Journal of Physical and Chemical Reference Data, 1985) 1856.
7. B.-S. You, W.-W. Park, and I.-S. Chung, "The effect of Calcium additions on the oxidation behavior in Magnesium Alloys," *Scripta Mater.*, 42 (2000), 1089-1094.
8. J.-K. Lee, S. K. Kim, "Effect of CaO composition on oxidation and burning behaviors of AM50 Mg alloy," *Trans. Nonferrous Met. Soc. China*, 21 (2011), 23-27.
9. J.-K. Lee, S. K. Kim, "Effect of CaO Addition on the Ignition Resistance of Mg-Al Alloys," *Trans. Nonferrous Met. Soc. China*, 52 (2011), 1483-1488.
10. K. V. Gourishankar, M. K. Ranjbar, and G. R. St. Pierre, "Revision of the enthalpies and gibbs energies of formation of calcium oxide and magnesium oxide," *J. Phase Equilib.*, 14 (5) (1993), 601-611.
11. O. Kubaschewski, C.B. Alcock, and P.J. Spencer. *Metallurgical thermochemistry: 6th Edition* (Pergamon Press, Oxford) 376.
12. M. W. Chase, *NIST-JANAF Thermochemical Tables 4th Edition, Monograph 9 (Part I and Part II)* (Journal of Physical and Chemical Reference Data, 1998) 1951.
13. M. Binnewies, E. Milke, *Thermochemical Data of Elements and Compounds, 2nd ed.*, (Wiley-VCH, Weinheim, 2002) 928.
14. SGSub substances database, version 13.1, 2013, Scientific Group Thermodata Europe (SGTE), Saint Martin d'Hères, France.
15. Factsage substances database, FactPS-2013, (www.crct.polymtl.ca/fact/documentation)
16. W. Huang, M. Hillert, and X. Wang, "Thermodynamic assessment of the CaO-MgO-SiO₂ system," *Metall. Mater. Trans.* 26 (A) (1995), 2293-2310.
17. K. Balewski et al., PETRA III: A New High Brilliance Synchrotron Radiation Source At DESY, Proceedings of EPAC 2004 (2004), 2302-2304.
18. Deutsche Elektronen-Synchrotron DESY, <http://photon-science.desy.de> (2014)
19. P. Villars and K. Cenzual, *Pearson's Crystal Data - Crystal Structure Database for Inorganic Compounds*, (on CD-ROM), Release 2013/14, ASM International (2014)
20. PanMg database, Computherm LLC, Madison, WI, (www.computherm.com)
21. A. Kozlov and R. Schmid-Fetzer, to be published.
22. W. Cao et al., "PANDAT Software with PanEngine, PanOptimizer and PanPrecipitation for Materials Property Simulation of Multi-Component Systems," *Calphad*, 33 (2009), 328-342.